INL/CON-16-40261
PREPRINT

Channel Estimation for Filter Bank Multicarrier Systems in Low SNR Environments

IEEE International Conference on Communications (ICC-2017)

Jonathan Driggs, Taylor Sibbett,
Hussein Moradiy, Behrouz Farhang-Boroujeny

May 2017

The INL is a
U.S. Department of Energy
National Laboratory
operated by
Battelle Energy Alliance

Channel Estimation for Filter Bank Multicarrier Systems in Low SNR Environments

Jonathan Driggs*, Taylor Sibbett*, Hussein Moradi† and Behrouz Farhang-Boroujeny*
*Department of Electrical and Computer Engineering
University of Utah, Salt Lake City, UT 84112
†Idaho National Laboratory
Idaho Falls, ID 83415

***Abstract*—Channel estimation techniques are crucial for reliable communications. This paper is concerned with channel estimation in a filter bank multicarrier spread spectrum (FBMC-SS) system. We explore two channel estimator options: (i) a method that makes use of a periodic preamble and mimics the channel estimation techniques that are widely used in OFDM-based systems; and (ii) a method that stays within the traditional realm of filter bank signal processing. For the case where the channel noise is white, both methods are analyzed in detail and their performance is compared against their respective Cramer-Rao Lower Bounds (CRLB). Advantages and disadvantages of the two methods under different channel conditions are given to provide insight to the reader as to when one will outperform the other.**

I. Introduction

Filter bank multicarrier (FBMC) has been proposed as a desirable alternative to orthogonal frequency division multiplexing (OFDM) in applications where spectral efficiency and spectral mobility are important [1]. A special class of spread spectrum waveforms that are built based on FBMC (FBMC-SS) was introduced in [2]. It was noted that FBMC-SS offers robust performance in high noise and high interference applications. The robustness of the FBMC-SS can be attributed to the recombining of the spread data symbols in the receiver though the principle of maximum ratio combining (MRC), which naturally filters out those portions of the spectrum that have received a high level of interference. The combining equation requires a reasonable estimate of the communications channel, which motivated the study and development of the channel estimation algorithms presented in this paper.

The problem of estimating the channel has been well studied in OFDM literature. The presence of the cyclic prefix (CP) in OFDM introduces a periodicity in its waveform which in turn leads to channel estimators that easily achieve the CRLB [3]. The CP absorbs the channel transient and the samples of a single OFDM symbol contain sufficient information that can provide an unbiased estimate of the channel frequency response at N equally spaced frequency points, where N is the length of FFT in OFDM. When the number of pilot subcarriers is less than N, the channel estimates will be limited to the positions of the pilots. The first contribution of this paper is to show how the channel estimation methods that have been developed for OFDM-based system can be extended to FBMC-based systems. This method is referred to as the *OFDM-like ML channel estimator* in this paper.

In filter bank literature, many channel estimation methods are based on the assumption that the channel over each subcarrier band can be approximated by a flat-gain [2], [4], [5]. Additional measures/steps for improving the channel estimate have also been explored for OFDM that can be applied to filter bank systems, e.g., the transform-domain noise reduction techniques [6]–[8]. Nevertheless, several works assert that the flat-gain assumption in many cases may be too coarse and thus alternative methods such as per-subcarrier multi-tap equalization [9] have to be sought. In the second part of this paper, we examine the flat-gain assumption in FBMC channel estimation and provide a detailed mathematical comparison of its performance to the approximation-free channel estimator that is presented in the first part of the paper. This second method is referred to as the *flat-gain ML channel estimator*. The results of both channel estimators are bench-marked against the CRLB. We find that our proposed approximation-free channel estimator performs at the CRLB regardless of the frequency selectivity of the channel, whereas the channel estimator that assumes a flat channel gain across each subcarrier is limited by the delay spread of the channel.

The rest of the paper is organized as follows. Section II provides a brief introduction to the FBMC-SS waveform and describes the structure of the pilot symbols used for channel estimation. Section III derives the maximum likelihood channel estimator for an OFDM-inspired algorithm and the maximum likelihood channel estimator formulated with the flat gain assumption. Section IV derives expressions for the mean square error for both channel estimation algorithms in order to provide a quantitative measure of their performance. Section V-A derives the CRLB for each estimation algorithm and relates the bound to the mean square error expression

This manuscript has been authored by Battelle Energy Alliance, LLC under Contract No. DE-AC07-05ID14517 with the U.S. Department of Energy. The United States Government retains and the publisher, by accepting the paper for publication, acknowledges that the United States Government retains a nonexclusive, paid-up, irrevocable, world-wide license to publish or reproduce the published form of this manuscript, or allow others to do so, for United States Government purposes. STI Number: INL/CON-16-40261

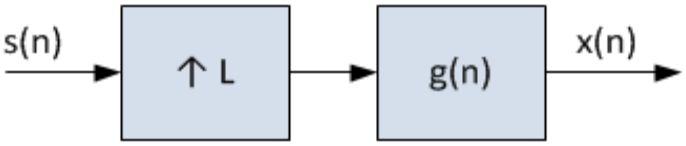

Fig. 1. FBMC-SS Transmitter Model

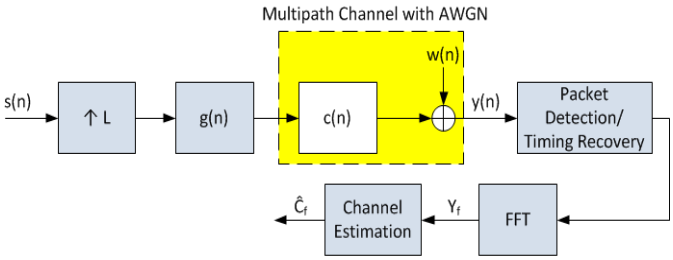

Fig. 2. System Model for the OFDM-Like channel estimator

for each estimator. Section VI presents simulated results of the described methods and confirms the theoretical work developed in this paper. Concluding remarks are given in section VII.

II. FBMC-SS Signal Model

FBMC-SS builds its waveform using a filter bank consisting of many subcarriers. The case of interest is this paper is when the same data symbol is spread across all of the subcarriers [2]. In this case, the transmitter baseband processing can be simplified to the one presented in Fig. 1. The transmit data symbols are up-sampled by a factor of L and passed through a synthesis filter bank $g(n)$ with N active subcarriers. Accordingly, the synthesized transmit signal can be expressed as

$$x(n) = \sum_{m} s(m) g(n - mL) \tag{1}$$

where $s(m)$ are data symbols. At the beginning of each data packet, $s(m)$ is replaced by a sequence of training/pilot symbols, $a(m)$, that will be used for packet detection and channel estimation.

In this paper, we assume $a(m)$ is a periodic sequence with a period of K. When this sequence is up-sampled by a factor of L and passed through $g(n)$, the result, after passing through its transient period, will be a sequence with a period of LK samples. Periodicity of this signal implies that it is a summation of LK complex sine waves with frequencies $f_k = \frac{2\pi k}{LK}$ for $k = 0, 1, \cdots, LK-1$. This mathematically is written as

$$\tilde{x}(n) = \frac{1}{\sqrt{LK}} \sum_{k=0}^{LK-1} \widetilde{X}(k) e^{j\frac{2\pi kn}{LK}} \tag{2}$$

where $\tilde{x}(n)$ is the periodic part of $x(n)$ that arises from the periodic preamble $a(m)$, and $\widetilde{X}(k)$ are the Fourier series coefficients of $\tilde{x}(n)$.

The derivations in the rest of this paper will be greatly simplified through use of a set of vectors and matrices. With this regard, here, we define the column vectors

$$\mathbf{x} = \begin{bmatrix} \tilde{x}(0) \\ \tilde{x}(1) \\ \vdots \\ \tilde{x}(LK-1) \end{bmatrix} \quad \text{and} \quad \mathbf{x}_{\mathrm{f}} = \begin{bmatrix} \widetilde{X}(0) \\ \widetilde{X}(1) \\ \vdots \\ \widetilde{X}(LK-1) \end{bmatrix}.$$

Here, and the rest of this paper, we adhere to the notation of using bold lower case for column vectors and add the subscript 'f' when a vector carries a set of frequency domain samples. We also note the $\mathbf{x}$ and $\mathbf{x}_{\mathrm{f}}$ are related according to the equation

$$\mathbf{x}_{\mathrm{f}} = \boldsymbol{\mathcal{F}}\mathbf{x} \tag{3}$$

where $\boldsymbol{\mathcal{F}}$ is the normalized discrete Fourier transform (DFT) matrix such that $\boldsymbol{\mathcal{F}}^{\mathrm{H}}\boldsymbol{\mathcal{F}} = \mathrm{I}$.

The DFT of the transmitted samples $\mathbf{x}_{\mathrm{f}}$ will be represented as a diagonal matrix when presenting an equation for the system model. The diagonal matrix, $\mathbf{X}_{\mathrm{f}}$, is related to $\mathbf{x}_{\mathrm{f}}$ according to the equation

$$\mathbf{X}_{\mathrm{f}} = \mathrm{diag}\left(\boldsymbol{\mathcal{F}}\mathbf{x}\right) \tag{4}$$

where $\mathrm{diag}(\cdot)$ refers to forming a diagonal matrix with the indicated elements.

III. Channel Estimation

A. OFDM-Like ML Channel Estimator

After the transmitted signal passes through a channel and leaves the corresponding transient period behind, the periodic sequence $\tilde{x}(n)$ leads to a periodic received signal with the same period. The result, when expressed in the form of a Fourier series expansion, has the following form:

$$\tilde{y}(n) = \frac{1}{KL} \sum_{k=0}^{KL-1} C(k) \widetilde{X}(k) e^{j\frac{2\pi kn}{KL}} + w(n) \tag{5}$$

where the factors $C(k)$ are the channel frequency response samples at the frequencies f_k and $w(n)$ is the channel noise. Note that $w(n)$ is, in general, an aperiodic sequence.

Taking a single period of $\tilde{y}(n)$ and applying a DFT to it, the result in the frequency domain may be written as

$$\mathbf{y}_{\mathrm{f}} = \mathbf{X}_{\mathrm{f}}\mathbf{c}_{\mathrm{f}} + \mathbf{w}_{\mathrm{f}} \tag{6}$$

where $\mathbf{c}_{\mathrm{f}}$ is a column vector with elements $C(0), C(1), \cdots, C(KL-1)$, and definitions of $\mathbf{y}_{\mathrm{f}}$ and $\mathbf{w}_{\mathrm{f}}$ should be clear from the context. The goal here is to find and estimate the unknown vector $\mathbf{c}_{\mathrm{f}}$ from (6).

Equation (6) has the familiar form of a linear model (see [10], Chapter 7). Accordingly, assuming $\mathbf{w}_{\mathrm{f}}$ has a proper complex Gaussian distribution with covariance matrix $\boldsymbol{\Sigma}$, (6) leads to the ML estimate

$$\widehat{\mathbf{c}}_{\mathrm{f}} = (\mathbf{X}_{\mathrm{f}}^{\mathrm{H}}\boldsymbol{\Sigma}^{-1}\mathbf{X}_{\mathrm{f}})^{-1}\mathbf{X}_{\mathrm{f}}^{\mathrm{H}}\boldsymbol{\Sigma}^{-1}\mathbf{y}_{\mathrm{f}}. \tag{7}$$

This portion needs to be rewritten The above derivations assume that the duration of the channel impulse response (in the time domain) is less than a period of $\tilde{x}(n)$ (KL samples), but does not take any advantage of it to improve the channel estimate. Many wireless channels encountered in practice have a duration of at most 1 or 2 μs, e.g., see [11]–[13]. But, for typical designs and, particularly, the case of interest in this paper, a period of $x_p(n)$ may be one or two orders of magnitudes longer. Making use of this information reduces the MSE of the channel estimate by the same factor; i.e., orders of magnitude improvement in the channel estimates is possible. Such improved channel estimates are obtained by adding the following modification to the previous formulations.

Let $\mathbf{c}$ be a length $L_{\rm c} < KL$ column vector denoting the channel impulse response in the time domain. The frequency domain channel response $\mathbf{c}_{\rm f}$ is obtained from $\mathbf{c}$ by appending $KL - L_{\rm c}$ zeros (to extend its length to KL) and applying a DFT to the result. Equivalently, $\mathbf{c}_{\rm f}$ can be obtained by

$$\mathbf{c}_f = \boldsymbol{\mathcal{F}}_{\rm p}\mathbf{c} \tag{8}$$

where $\boldsymbol{\mathcal{F}}_{\rm p}$ is a partial DFT matrix containing the first $L_{\rm c}$ columns of $\boldsymbol{\mathcal{F}}$.

Replacing (8) in (6), we get new linear equation from which we obtain the ML estimate of $\mathbf{c}$ as

$$\widehat{\mathbf{c}}_{\rm D} = ((\mathbf{X}_{\rm f}\boldsymbol{\mathcal{F}}_{\rm p})^{\rm H}\boldsymbol{\Sigma}^{-1}\mathbf{X}_{\rm f}\boldsymbol{\mathcal{F}}_{\rm p})^{-1}(\mathbf{X}_{\rm f}\boldsymbol{\mathcal{F}}_{\rm p})^{\mathbf{H}}\boldsymbol{\Sigma}^{-\mathbf{1}}\mathbf{y}_{\rm f}, \tag{9}$$

where the subscript D has been added to indicate that this is a 'denoised' estimate of the channel. Taking the DFT of $\widehat{\mathbf{c}}_{\rm D}$ leads to the improved estimate

$$\widehat{\mathbf{c}}_{\rm f,D} = \boldsymbol{\mathcal{F}}_{\rm p}\widehat{\mathbf{c}}. \tag{10}$$

B. Flat-Gain FBMC ML Channel Estimator

The estimator in this subsection makes the assumption that the channel frequency response is flat across each of the N total subcarriers. We also assume that the combination of the transmitter pulse-shaping filter and its match at the receiver makes a perfect Nyquist filter. The matched filter in this case corresponds to the analysis filter bank, which has the structure defined in [2, Fig. 13]. With these assumptions and noting that the pilot subcarriers are non-overlapping, the pilot symbols will be affected by the channel gains (the samples of channel frequency response) at the respective subcarriers. In the sequel, we use this property to develop the flat-gain ML channel estimator.

A system model depicting the placement of the flat-gain ML Channel Estimator is shown in Fig. 3. The matched filtered data out of the analysis filter bank's kth subcarrier can be written as

$$z_k(n) = C_k a_k(n) + v_k(n). \tag{11}$$

where $a_k(n)$ are the pilots symbols that are known to the receiver. Also, in Fig. 3, the packet detection and timing recovery block assures that the receiver is correctly aligned with the pilot symbols. Note that, in (11), k is the subcarrier index corresponding to frequency f_k and n is the time index

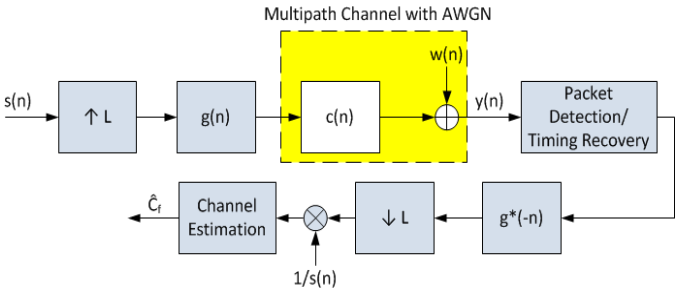

Fig. 3. System Model for the flat-gain channel estimator

of the pilot symbols. Moreover, $v_k(n)$ are samples originating from the channel noise.

For estimating the channel at each subcarrier, we refer to (11) and note that $a_k(n)$ is known to the receiver. Therefore, we can multiply the received symbol by the inverse of $a_k(n)$ to obtain

$$z'_k(n) = C_k + v'_k(n), \tag{12}$$

where $z'_k(n) = z_k(n)/a_k(n)$ and $v'_k(n) = v_k(n)/a_k(n)$. Assuming that the channel noise is Gaussian and white, the use of a square-root Nyquist filter at the receiver input implies that the noise samples $v'_k(n)$, for $n = 0, 1, \cdots, K-1$, are Gaussian and uncorrelated. Furthermore, if we assume that $|a(k)| = 1$, one will find the noise samples $v'_k(n)$ are independent and identically distributed for all values k and n. We use σ_v^2 to denote the variance of these samples.

Next considering the form of (12), for each choice of m and $k = 0, 1, \cdots, K-1$, the minimum-variance unbiased (MVUB) estimator of $C(m)$ is obtained as [10]

$$\widehat{C}_k = \frac{1}{M}\sum_{n=1}^{M} z'_k(n). \tag{13}$$

Obviously, this estimate has a mean value of C_k and variance σ_k^2/M, which implies the variance of the estimate C_k decreases as M increases.

Additionally, no assumption about the finite duration of the channel has been made. If the same assumption about the channel impulse response being constrained to a finite length $L_{\rm c}$ is made as for the OFDM-Like ML Estimator, an algorithm can be developed to only retain useful channel information and remove noise information in the time domain.

The estimated impulse response in the FBMC-SS receiver exists in an N-dimensional subspace, where N is the number of subcarriers used. This N-dimensional subspace corresponds to a limitation in time to $1/f_0$ seconds, where f_0 represents the distance in Hz of adjacent subcarriers. Additionally, the additive white noise introduced in the channel exists in the sampled N-dimensional subspace. If $L_{\rm c}$ is less than N, the N impulse response samples can be projected onto the $L_{\rm c}$-dimensional subspace to remove noise without any loss of channel impulse response information.

Our denoising algorithm begins by taking the IDFT of the scaled received filter bank output across all subcarriers at time n, which is denoted as

$$\mathbf{z}'' = \boldsymbol{\mathcal{F}}^{-1}\mathbf{c}_{\mathrm{f}} + \boldsymbol{\mathcal{F}}^{-1}\mathbf{v}, \tag{14}$$

where the vectors $\mathbf{c}_{\mathrm{f}}$ and $\mathbf{v}$ represent the channel and noise components across all N subcarriers at time n, and $\boldsymbol{\mathcal{F}}^{-1}$ is the inverse DFT matrix. To remove a portion of the noise, the data is multiplied by an orthogonal projection matrix $\mathbf{P}_{\mathrm{c}}$ that projects the data onto the subspace of the channel impulse response. The form of $\mathbf{P}_c$ is simply a diagonal matrix of ones that has zeros in the last $N - L_{\mathrm{c}}$ diagonal entries, giving the denoised time vector

$$\mathbf{z}_{t,D} = \boldsymbol{\mathcal{F}}^{-1}\mathbf{c}_{\mathrm{f}} + \mathbf{P}_{\mathrm{c}}\boldsymbol{\mathcal{F}}^{-1}\mathbf{v}. \tag{15}$$

The product of the projection matrix $\mathbf{P}_{\mathrm{c}}$ and the channel impulse response is simply the channel impulse response in (15), which results in only the noise term being affected by the projection. The information can be transformed back to the frequency domain by multiplying by a DFT matrix, leaving

$$\mathbf{z}_{\mathrm{D}} = \mathbf{c}_{\mathrm{f}} + \boldsymbol{\mathcal{F}}\mathbf{P}_{\mathrm{c}}\boldsymbol{\mathcal{F}}^{-1}\mathbf{v}. \tag{16}$$

In order to quantify the effects of the projection operation on the noise power, let us assume that $\sigma_{\mathrm{k}}^2 = \sigma^2$ for all values of k. The probability density function of (16) can be written as:

$$\begin{aligned} P(\mathbf{z}_{\mathrm{D}}, \sigma^2) &\sim \mathcal{CN}(\mathbf{c}_{\mathrm{f}}, \sigma^2\boldsymbol{\mathcal{F}}\mathbf{P}_{\mathrm{c}}\boldsymbol{\mathcal{F}}^{-1}) \\ &\sim \mathcal{CN}(\mathbf{c}_{\mathrm{f}}, \sigma^2\boldsymbol{\Sigma}_{\mathrm{D}}). \end{aligned} \tag{17}$$

The covariance matrix in (17) can be interpreted as the IDFT of a truncated DFT matrix. The rows of the truncated DFT matrix contain frequency shifted rectangular windows, and taking the IDFT results in a circulant matrix containing

$$\boldsymbol{\Sigma}_{\mathrm{D,(k,i)}} = \frac{1}{N}\frac{\sin(\frac{\pi L_{\mathrm{c}}(i-k)}{N})}{\sin(\frac{\pi(i-k)}{N})}\exp^{\frac{2\pi j(i-k)(L_{\mathrm{c}}-1)}{2N}}. \tag{18}$$

L'Hospital's rule can be used to evaluate the diagonal elements of the covariance matrix as

$$\boldsymbol{\Sigma}_{\mathrm{D,(k=i)}} = \frac{1}{N}\lim_{\mathrm{(k-i)}\to 0}\frac{\sin(\frac{\pi L_{\mathrm{c}}(0)}{N})}{\sin(\frac{\pi(0)}{N})} = \frac{L_{\mathrm{c}}}{N}. \tag{19}$$

The denoising process removes noise from the impulse response estimate derived from a single FBMC-SS symbol. The resulting channel estimate has a covariance $\boldsymbol{\Sigma}_{\mathrm{D}}$, which is described in (18). If M successive FBMC-SS symbols are denoised and averaged, we form the flat-gain channel estimator. The PDF of this channel estimator is given below as

$$\widehat{\mathbf{c}}_{\mathrm{f,D}} \sim \mathcal{CN}\left(\mathbf{c}_{\mathrm{f}}, \frac{\sigma^2}{M}\boldsymbol{\Sigma}_{\mathrm{D}}\right). \tag{20}$$

IV. Performance Analysis

The performance of the two channel estimators can be expressed in terms of total mean square error (MSE). It will be shown that the ML estimator derived under the flat-gain assumption achieves similar performance to the OFDM-like ML Estimator under various conditions. When the flat-gain ML Estimator achieves does not achieve similar performance, it can be attributed to two factors. In [7], it was noted that the DFT of samples with non-integer timing intervals will result in spectral leakage. The spectral leakage introduced by non-ideal sample timing will spread out the energy of the channel impulse response, and some of the dispersed energy will be truncated by the denoising operation. Additionally, the flat-gain ML Estimator will become increasingly biased as the coherence bandwidth of the channel frequency response decreases.

A. OFDM-Like MLE Performance

To derive an expression for the OFDM-like channel estimator's MSE, we first will prove that the ML channel estimator derived in Section III-A is unbiased. Starting with (9), and denoting $\mathbf{Z} = \boldsymbol{\mathcal{F}}_{\mathrm{p}}((\mathbf{X}_{\mathrm{f}}\boldsymbol{\mathcal{F}}_{\mathrm{p}})^{\mathbf{H}}\boldsymbol{\Sigma}^{-\mathbf{1}}\mathbf{X}_{\mathrm{f}}\boldsymbol{\mathcal{F}}_{\mathrm{p}})^{-\mathbf{1}}(\mathbf{X}_{\mathrm{f}}\boldsymbol{\mathcal{F}}_{\mathrm{p}})^{\mathbf{H}}\boldsymbol{\Sigma}^{-\mathbf{1}}$, the probability distribution of the MLE has a mean

$$E[P(\widehat{\mathbf{c}}_{ML,f})] = \mathbf{Z}\mathbf{X}_{\mathrm{f}}\boldsymbol{\mathcal{F}}_{\mathrm{p}}\mathbf{c}_{\mathrm{p}} \tag{21}$$

and covariance

$$\mathrm{cov}[P(\widehat{\mathbf{c}}_{ML,f})] = \mathbf{Z}\Sigma\mathbf{Z}^{H}. \tag{22}$$

By eliminating terms in the mean and covariance expressions, the Gaussian PDF can be simplified to

$$\begin{aligned} P(\widehat{\mathbf{c}}_{ML,f}) \sim \mathcal{CN}\Bigg(&\boldsymbol{\mathcal{F}}_{\mathrm{p}}\mathbf{c}_{\mathrm{p}}, \\ &\boldsymbol{\mathcal{F}}_{\mathrm{p}}((\mathbf{X}_{\mathrm{f}}\boldsymbol{\mathcal{F}}_{\mathrm{p}})^{\mathbf{H}}\boldsymbol{\Sigma}^{-\mathbf{1}}\mathbf{X}_{\mathrm{f}}\boldsymbol{\mathcal{F}}_{\mathrm{p}})^{-\mathbf{1}}\boldsymbol{\mathcal{F}}_{\mathrm{p}}^{\mathbf{H}}\Bigg). \end{aligned} \tag{23}$$

The mean of the probability density function in (23) is the channel frequency response. Therefore, the estimator is unbiased. The MSE of this unbiased estimator is expressed as

$$\mathbf{MSE} = E\left((\widehat{\mathbf{c}}_{\mathrm{f}} - \mathbf{c}_{\mathrm{f}})^{\mathrm{H}}(\widehat{\mathbf{c}}_{\mathrm{f}} - \mathbf{c}_{\mathrm{f}})\right) \tag{24}$$

The expression in (24) is simply the sum of the variances of the estimator. If the additive noise is white and Gaussian with variance σ^2, the covariance of the ML estimator can be expressed as

$$cov(\widehat{\mathbf{c}}_{\mathbf{ML,f}}) = \sigma^2\boldsymbol{\mathcal{F}}_{\mathrm{p}}(\boldsymbol{\mathcal{F}}_{\mathrm{p}}^{H}\mathbf{X}_{\mathrm{f}}^{\mathbf{H}}\mathbf{X}_{\mathrm{f}}\boldsymbol{\mathcal{F}}_{\mathrm{p}})^{-\mathbf{1}}\boldsymbol{\mathcal{F}}_{\mathrm{p}}^{\mathbf{H}}. \tag{25}$$

Given that the estimator is unbiased, the MSE can be computed using the covariance matrix in (25).

$$\mathbf{MSE} = tr\left[\sigma^2\boldsymbol{\mathcal{F}}_{\mathrm{p}}(\boldsymbol{\mathcal{F}}_{\mathrm{p}}^{\mathrm{H}}\mathbf{X}_{\mathrm{f}}^{\mathbf{H}}\mathbf{X}_{\mathrm{f}}\boldsymbol{\mathcal{F}}_{\mathrm{p}})^{-\mathbf{1}}\boldsymbol{\mathcal{F}}_{\mathrm{p}}^{\mathbf{H}}\right]. \tag{26}$$

It will be shown in the following section that the mean square error corresponds to the CRLB.

B. Flat-Gain MLE Performance

The probability distribution of the flat-gain ML Estimator was derived in (20). Additionally, the estimator was established to be theoretically unbiased if the flat-gain assumption holds. However, as noted in the introduction to this section, there are several practical conditions that will introduce a bias. The practical bias will be represented by the error term ϵ in the following equations. Using the fact that the estimator is theoretically unbiased, the total MSE of the flat-gain ML Estimator is computed as

$$\begin{aligned}\mathbf{MSE} &= E\left((\widehat{\mathbf{c}}_{\mathrm{f,D}} - \mathbf{c}_{\mathrm{f}})^{\mathrm{H}}(\widehat{\mathbf{c}}_{\mathrm{f,D}} - \mathbf{c}_{\mathrm{f}})\right) \\ &= tr\left[\frac{\sigma^2}{M}\mathbf{\Sigma}_D\right] + \epsilon = \frac{L_{\mathrm{c}}\sigma^2}{M} + \epsilon \end{aligned} \tag{27}$$

V. Cramer-Rao Lower Bound Derivation

A common metric for estimators is the CRLB, which provides a lower bound on the variance of any unbiased estimator. We proceed to derive the CRLB for both channel estimation methods in the following subsections and compare the results to each estimator.

A. CRLB for the OFDM-Like Formulation

In this section, we compute the CRLB for the OFDM-like ML estimator and show that it is efficient, which means that it achieves the CRLB. In order to reduce the complexity of the derivation for the CRLB, we choose to compute the CRLB for estimating the impulse response vector $\mathbf{c}_{\mathrm{p}}$. To relate the CRLB for the impulse response estimate to the frequency domain estimate, we note that the efficiency of estimators is maintained over linear transformations [10, p. 37], [3]. Therefore, the objective of this section is to relate the IDFT of the channel frequency response estimate in (9) to the time domain CRLB. Once it is shown that the channel impulse response estimator's covariance matrix corresponds to the CRLB, the frequency domain channel estimator is proven to meet the CRLB because it is a linear transformation of the time domain estimate. Starting with the PDF of the receiver input data defined in (6) and assuming the channel impulse response has a finite length where $\mathbf{c}_f = \boldsymbol{\mathcal{F}}_{\mathrm{p}}\mathbf{c}_{\mathrm{p}}$, the score function is

$$\begin{aligned}\frac{\partial ln(P(\mathbf{Y}_f;\mathbf{c}_{\mathrm{p}}))}{\partial \mathbf{c}_{\mathrm{p}}} = -\frac{1}{2}\Big[&- 2\boldsymbol{\mathcal{F}}_{\mathrm{p}}\mathbf{X}_{\mathrm{f}}^{\mathbf{H}}\mathbf{\Sigma}^{-\mathbf{1}}\mathbf{Y}_{\mathbf{f}} + \\ &2\boldsymbol{\mathcal{F}}_{\mathrm{p}}^{H}\mathbf{X}_{\mathrm{f}}^{\mathbf{H}}\mathbf{\Sigma}^{-\mathbf{1}}\mathbf{X}_{\mathrm{f}}\boldsymbol{\mathcal{F}}_{\mathrm{p}}\mathbf{c}_{\mathrm{p}}\Big]. \end{aligned} \tag{28}$$

From (28), the Hessian of the score function can be computed as

$$\frac{\partial^2 ln(P(\mathbf{Y}_f;\mathbf{c}_{\mathrm{p}}))}{\partial \mathbf{c}_{\mathrm{p}}\partial {\mathbf{c}_{\mathrm{p}}}^H} = -\boldsymbol{\mathcal{F}}_{\mathrm{p}}^{H}\mathbf{X}_{\mathrm{f}}^{\mathbf{H}}\mathbf{\Sigma}^{-\mathbf{1}}\mathbf{X}_{\mathrm{f}}\boldsymbol{\mathcal{F}}_{\mathrm{p}}. \tag{29}$$

The Fisher Information Matrix $\mathbf{F}(\mathbf{c}_{\mathrm{p}})$ is derived from the Hessian as

$$\begin{aligned}\mathbf{F}(\mathbf{c}_{\mathrm{p}}) &= -E\left[\frac{\partial^2 ln(P(\mathbf{Y}_f;\mathbf{c}_{\mathrm{p}}))}{\partial \mathbf{c}_{\mathrm{p}}\partial {\mathbf{c}_{\mathrm{p}}}^H}\right] \\ &= (\mathbf{X}_{\mathrm{f}}\boldsymbol{\mathcal{F}}_{\mathrm{p}})^{\mathbf{H}}\mathbf{\Sigma}^{-\mathbf{1}}\mathbf{X}_{\mathrm{f}}\boldsymbol{\mathcal{F}}_{\mathrm{p}}. \end{aligned} \tag{30}$$

An estimator meets the CRLB if it satisfies the following relation between its covariance matrix and the Fisher Information Matrix:

$$\mathbf{\Sigma}_{\widehat{\mathbf{c}}_{\mathrm{p}}} = \frac{1}{\mathbf{F}(\mathbf{c}_{\mathrm{p}})}. \tag{31}$$

In order to compute the covariance matrix of the time domain channel estimate, we begin by taking the IDFT of (9):

$$\widehat{\mathbf{c}}_{\mathrm{p}} = \boldsymbol{\mathcal{F}}_{\mathrm{p}}^{-1}\widehat{\mathbf{c}}_{\mathrm{f}}. \tag{32}$$

The equation in (32) is simply the product of a complex Gaussian vector with a linear operator, which results in the following PDF:

$$\begin{aligned} P(\widehat{\mathbf{c}}_{\mathrm{p}}, \mathbf{c}) &\sim \mathcal{CN}\Big(\boldsymbol{\mathcal{F}}_{\mathrm{p}}^{-1}\boldsymbol{\mathcal{F}}_{\mathrm{p}}\mathbf{c}_p, \\ &\qquad \boldsymbol{\mathcal{F}}_{\mathrm{p}}^{-1}\boldsymbol{\mathcal{F}}_{\mathrm{p}}((\mathbf{X}_{\mathrm{f}}\boldsymbol{\mathcal{F}}_{\mathrm{p}})^{\mathbf{H}}\mathbf{\Sigma}^{-\mathbf{1}}\mathbf{X}_{\mathrm{f}}\boldsymbol{\mathcal{F}}_{\mathrm{p}})^{-\mathbf{1}}\boldsymbol{\mathcal{F}}_{\mathrm{p}}^{\mathbf{H}}(\boldsymbol{\mathcal{F}}_{\mathrm{p}}^{-\mathbf{1}})^{\mathbf{H}}\Big) \\ &\sim \mathcal{CN}\Big(\mathbf{c}_{\mathrm{p}}, \left((\mathbf{X}_{\mathrm{f}}\boldsymbol{\mathcal{F}}_{\mathrm{p}})^{\mathbf{H}}\mathbf{\Sigma}^{-\mathbf{1}}\mathbf{X}_{\mathrm{f}}\boldsymbol{\mathcal{F}}_{\mathrm{p}}\right)^{-\mathbf{1}}\Big)\Big). \end{aligned} \tag{33}$$

The covariance matrix of the channel impulse estimate in (33) clearly satisfies the relationship defined in (31). Additionally, the time domain estimator remains unbiased. Therefore, the OFDM-like channel estimator achieves the CRLB.

B. CRLB For the Flat-Gain Formulation

In this section, we show that the flat-gain ML channel estimator derived in (20) achieves the CRLB if the flat-gain assumption is true. In addition to performing the standard derivation for the CRLB, we note that the expression for mean square error for the flat-gain ML estimator should be conditioned by the known length of the channel impulse response L_{c}. In the time domain, this conditioning can be expressed as limiting the noise to only the samples that corrupt the impulse response samples $c(n)$ in the range $0 \leq n \leq L_{\mathrm{c}} - 1$, which reduces the noise power by a factor L_{c}/N for a white noise environment. Relating this result to the frequency domain noise process, we note the the statistics of the white noise don't change in the frequency domain and the variance of the noise at each subcarrier is also scaled by L_{c}/N. Starting by writing the conditional PDF as $p(\mathbf{z}'_{\mathrm{k}}, c_{\mathrm{f}}(f_{\mathrm{k}}) \mid len\{\mathbf{c}\} = L_{\mathrm{c}})$, the Fisher Information can be written as

$$\begin{aligned}\mathbf{I}(c_{\mathrm{f}}(f_{\mathrm{k}})) &= -E\left[\frac{\partial^2 ln(p(\mathbf{z}'_{\mathrm{k}}, c_{\mathrm{f}}(f_{\mathrm{k}}) \mid len\{\mathbf{c}\} = L_{\mathrm{c}}))}{\partial c_{\mathrm{f}}(f_{\mathrm{k}})\partial c^*_{\mathrm{f}}(f_{\mathrm{k}})}\right] \\ &= -E\left[-\frac{MN}{\sigma^2 L_{\mathrm{c}}}\right] = \frac{MN}{\sigma^2 L_{\mathrm{c}}}. \end{aligned} \tag{34}$$

The CRLB can be written in terms of the Fisher Information as

$$\begin{aligned} var(\widehat{c}_{\mathrm{f}}(f_{\mathrm{k}})) &\geq \frac{1}{\mathbf{I}(c_{\mathrm{f}}(f_{\mathrm{k}}))} \\ &\geq \frac{\sigma^2 L_{\mathrm{c}}}{MN}, \end{aligned} \tag{35}$$

where M is the number of samples used in the computation of the estimate. If the error term ϵ is zero in (27), it can

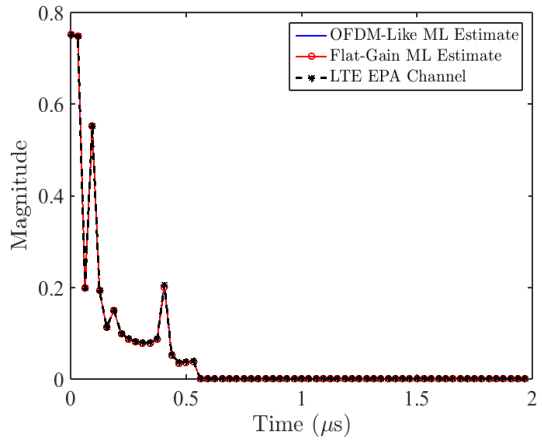

Fig. 4. Channel Impulse Response Estimates for LTE EPA 5 Hz channel at High SNR

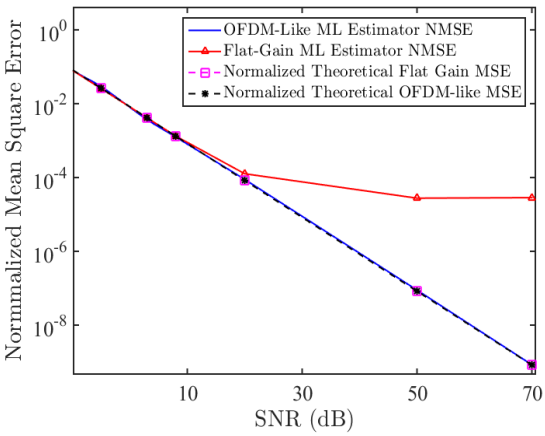

Fig. 5. NMSE vs. Received SNR for LTE EPA 5 Hz Multipath Channel

be seen that the flat-gain Channel Estimator meets the CRLB according to the following relation:

$$\frac{\sigma^2}{M}\left[\mathbf{\Sigma}_{\mathrm{D}}\right]_{\mathrm{ii}} = \left[\mathbf{I}^{-1}(\mathbf{c}_{\mathrm{f}})\right]_{\mathrm{ii}}. \tag{36}$$

However, we will show in the results section that the ϵ can have a significant effect on the MSE of the estimator.

VI. Results

In this section, we provide MATLAB simulation results to check the theoretical work developed in the previous sections and provide intuition for practical applications. The simulation configuration is given below:

i) Filter Bank Size = 128.
ii) Number of Active Subcarriers = 64.
iii) Periodic Pilot Sequence Length (K) = 16.
iv) The channel is static over the duration of the FBMC-SS Packet.
v) Pilot symbols are transmitted on all subcarriers during the preamble.
vi) The filter bank subcarrier spacing = 500 kHz.
vii) The channel length (L_{c}) is known *apriori* by the receiver for both estimation methods.
viii) White Gaussian noise is added to the channel output with the SNR swept from -10dB Es/No to 100dB Es/No.
ix) Perfect timing synchronization and carrier synchronization are assumed.
x) The transient introduced by the channel is absorbed by the beginning of the preamble during packet detection such that the estimate is performed on non-transient data.

In order to compare the relative performance of the estimators, we compute the Normalized Mean Square Error (NMSE) of each estimator using the following equation:

$$NMSE = \frac{(\widehat{\mathbf{c}}_{\mathrm{f}} - \mathbf{c}_{\mathrm{f}})^{\mathrm{H}}(\widehat{\mathbf{c}}_{\mathrm{f}} - \mathbf{c}_{\mathrm{f}})}{\mathbf{c}_{\mathrm{f}}^{\mathrm{H}}\mathbf{c}_{\mathrm{f}}}. \tag{37}$$

In order to quantify the measured NMSE, we proceed to normalize the theoretical expressions that met the CRLB.

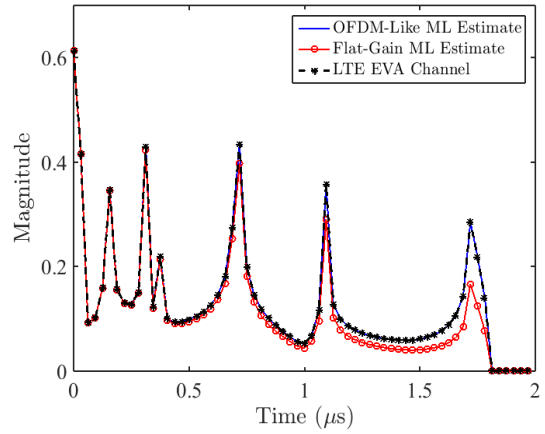

Fig. 6. Channel Impulse Response Estimates for LTE EVA 5 Hz channel at High SNR

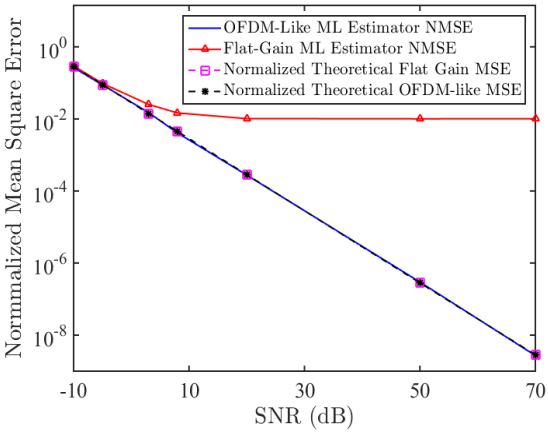

Fig. 7. NMSE vs. Received SNR for LTE EVA 5 Hz Channel

The theoretical MSE for the OFDM-like estimator in (26) is normalized according to the following equation:

$$NMSE_{\text{theory,OL}} = \frac{tr\left[\sigma^2 \boldsymbol{\mathcal{F}}_{\text{p}}(\boldsymbol{\mathcal{F}}_{\text{p}}^{\text{H}}\mathbf{X}_{\text{f}}^{\mathbf{H}}\mathbf{X}_{\text{f}}\boldsymbol{\mathcal{F}}_{\text{p}})^{-\mathbf{1}}\boldsymbol{\mathcal{F}}_{\text{p}}^{\mathbf{H}}\right]}{\mathbf{c}_{\text{f}}^{\text{H}}\mathbf{c}_{\text{f}}}. \tag{38}$$

Additionally, the flat-gain channel estimator's theoretical MSE in (27) is normalized as follows:

$$NMSE_{\text{theory,FG}} = \frac{tr\left[\frac{\sigma^2}{M}\boldsymbol{\Sigma}_D\right]}{\mathbf{c}_{\text{f}}^{\text{H}}\mathbf{c}_{\text{f}}}. \tag{39}$$

The NMSE measured in simulation is compared to the normalized theoretical MSE for each estimator.

Two different channel models are used to evaluate the OFDM-like channel estimator and the flat-gain channel estimator. The first channel model used is an LTE EPA channel with a Doppler frequency of 5Hz, as defined in [11]. The impulse response of the LTE EPA channel is shown alongside the impulse response estimates for the channel in Fig. 4. This channel model is time-limited to approximately 410 ns, which results in a larger coherence bandwidth in the frequency domain and increases the validity of the flat-gain assumption. To measure the accuracy of the flat-gain assumption and compare the performance of the estimators, the measured NMSE of the estimators and the theoretical NMSE for the estimators are shown in Fig. 5. It can be seen that the flat-gain channel estimator matches theory until the bias begins to dominate the NMSE at high SNR. The bias, modeled as ϵ in (27), is considered negligible in this scenario. Additionally, we note that the OFDM-like estimator does not suffer from any bias and matches theory across all SNR points. It is also worth noting that both theoretical NMSE curves are identical.

The second channel model used to evaluate the estimators is an LTE EVA channel with a Doppler frequency of 5Hz, as defined in [11]. We chose to use this channel model to illustrate the effectiveness of the estimators when the channel impulse response has a longer duration in time. In the comparison of the impulse response to the estimated impulse responses in Fig. 6, the bias of the flat-gain Channel Estimator is apparent. The stronger bias, dominated by the inaccuracy of the flat-gain assumption, is also reflected in the plot of the estimator NMSE in Fig. 7, where the NMSE floors at approximately 10^{-2}. These results show that the flat-gain Channel Estimator is an effective method for estimating time-limited channels, but has limited performance in urban environments where the channel delay spread is larger. On the other hand, the OFDM-like channel estimator is very effective for most practical channels.

VII. Conclusion

In this paper, we presented two maximum likelihood channel estimation schemes for FBMC-SS and evaluated their performance against the Cramer Rao Lower Bound. An OFDM-like channel estimator was derived that utilizes the tones generated by a periodic pilot sequence to estimate the channel frequency response, and it was shown through detailed analysis that this estimator meets the CRLB. A standard alternative channel estimation method, denoted as the flat-gain channel estimator, was analyzed and shown to also meet the CRLB when the assumptions surrounding the formulation of the estimator are valid. We provided simulation results that highlighted the validity of the flat-gain assumption for the flat-gain channel estimator using several LTE channel models, and confirmed that the flat-gain channel estimator only meets the CRLB for relatively time-limited channels at lower signal to noise ratio levels. On the other hand, the simulation results confirmed that the OFDM-like channel estimator maintains excellent performance across the different simulation conditions. Based on these results, we propose the flat-gain ML estimator as a good choice for applications where the channel delay spread is small and low computational complexity is desirable. For urban environments where the propagation channel becomes more diverse, the OFDM-like channel estimator is a superior choice. Our future work will focus on further developing the OFDM-like channel estimator by reducing its computational complexity and analyzing its performance in the presence of partial band interference.

References

[1] B. Farhang-Boroujeny, "OFDM versus filter bank multicarrier," *IEEE Signal Processing Magazine*, vol. 28, no. 3, pp. 92–112, 2011.

[2] D. Wasden, H. Moradi, and B. Farhang-Boroujeny, "Design and Implementation of an Underlay Control Channel for Cognitive Radios," *IEEE Journal on Selected Areas in Communications*, vol. 30, no. 10, pp. 1875–1889, 2012.

[3] M. Morelli and U. Mengali, "A comparison of pilot-aided channel estimation methods for OFDMsystems," *Signal Processing, IEEE Transactions on [see also Acoustics, Speech, and Signal Processing, IEEE Transactions on]*, vol. 49, no. 12, pp. 3065–3073, 2001.

[4] J.-p. Javaudin, D. Lacroix, and A. Rouxel, "Pilot-Aided Channel Estimation for OFDM / OQAM," in *Vehicular Technology Conference, 2003. VTC 2003-Spring. The 57th IEEE Semiannual*, 2003, pp. 1581–1585.

[5] D. Kong, D. Qu, and T. Jiang, "Time domain channel estimation for OQAM-OFDM systems: Algorithms and performance bounds," *IEEE Transactions on Signal Processing*, vol. 62, no. 2, pp. 322–330, 2014.

[6] Y. Zhao and A. Huang, "A Novel Channel Estimation Method for OFDM Mobile Communication Systems Based on Pilot Signals and Transform-Domain Processing," in *Vehicular Technology Conference, 1997, IEEE 47th*, 1997, pp. 2089–2093.

[7] M. Sandell and S. K. Wilson, "On Channel Estimation in OFDM Systems," in *Vehicular Technology Conference, 1995 IEEE 45th*, no. 1, 1995, pp. 815–819.

[8] H. Minn, S. Member, and V. K. Bhargava, "An Investigation into Time-Domain Approach for OFDM Channel Estimation," *IEEE TRANSACTIONS ON BROADCASTING*, vol. 46, no. 4, pp. 240–248, 2000.

[9] L. G. Baltar, M. Newinger, and J. A. Nossek, "Structured subchannel impulse response estimation for filter bank based multicarrier systems," *Proceedings of the International Symposium on Wireless Communication Systems*, pp. 191–195, 2012.

[10] S. M. Kay, *Fundamentals of Statistical Signal Processing: Estimation Theory*. Upper Saddle River, NJ, USA: Prentice-Hall, Inc., 1993.

[11] T. Specification, "Etsi ts 136 104," *(3GPP TS 36.101 version 10.3.0 Release 10*, vol. 0, 2011.

[12] Report ITU-R M.2135-1, "Guidelines for evaluation of radio interface technologies for IMTadvanced," *Evaluation*, vol. 93, no. 3, 2009. [Online]. Available: http://www.ncbi.nlm.nih.gov/pubmed/19923880

[13] P. Ö. Henrik Asplund, Kjell Larsson, "How typical is the " Typical Urban " channel model ?" in *Vehicular Technology Conference, 2008. VTC Spring 2008. IEEE*, 2008, pp. 340–343.